Gaussian Process Model for Collision Dynamics of Complex Molecules

Jie Cui and Roman V. Krems
Department of Chemistry, University of British Columbia, Vancouver, British Columbia V6T 1Z1, Canada

(Received 2 March 2015; published 13 August 2015)

We show that a Gaussian process model can be combined with a small number (of order 100) of scattering calculations to provide a multidimensional dependence of scattering observables on the experimentally controllable parameters (such as the collision energy or temperature) as well as the potential energy surface (PES) parameters. For the case of Ar-C_6H_6 collisions, we show that 200 classical trajectory calculations are sufficient to provide a ten-dimensional hypersurface, giving the dependence of the collision lifetimes on the collision energy, internal temperature, and eight PES parameters. This can be used for solving the inverse scattering problem, for the efficient calculation of thermally averaged observables, for reducing the error of the molecular dynamics calculations by averaging over the PES variations, and for the analysis of the sensitivity of the observables to individual parameters determining the PES. Trained by a combination of classical and quantum calculations, the model provides an accurate description of the quantum scattering cross sections, even near scattering resonances.

DOI: 10.1103/PhysRevLett.115.073202 PACS numbers: 34.10.+x, 34.20.Gj, 34.50.-s

Reliable scattering calculations of dynamical properties of molecules are required in almost any research field related to molecular physics. In particular, experiments on collisional cooling of molecules to cold and ultracold temperatures [1], chemical reaction dynamics [2], the development of new pressure standards [3,4], and astrophysics and astrochemistry [5] rely on accurate calculations of molecular collision cross sections. Currently, there are two major problems with the *ab initio* calculations of molecular dynamics observables. The first problem is the inaccuracy of the potential energy surfaces (PESs). Unfortunately, even the most sophisticated quantum chemistry calculations produce the PES with uncertainties that lead to significant (and often unknown) errors in the dynamical calculations. This sensitivity to PES inaccuracies is especially detrimental for low temperature applications (cold molecules, ultracold chemistry, astrophysics, and pressure standards) [6–8]. The second problem is related to the numerical complexity of the quantum dynamics calculations [9,10]. For complex molecules with many degrees of freedom, accurate dynamical calculations are extremely time consuming and it is often impossible to compute enough results for accurate averaging over the collision or internal energies of the colliding partners.

In the present work we propose a solution to these two problems. In order to account for the PES uncertainties, the dynamical results can be averaged over variations of the PES. If the computed observables are averaged over variations of each individual PES parameter, producing an expectation interval of the observables, the *ab initio* dynamical calculations can have fully predictive power (with error bars). However, the outcome of a molecular collision is generally a complicated function of many (ten or more) PES parameters. It is impossible to obtain the dependence of the collision observables on the individual PES parameters by the direct scattering calculations. We show that such a dependence can be obtained by a combination of a small number (on the order of 100) of scattering calculations with a Gaussian process (GP) model [11,12]. We show that the same model can be used to obtain the accurate dependence of the scattering observables on the collision or internal energies of the molecules, with a small number of scattering calculations. The result is an accurate global dependence of the scattering observables on the collision energy, internal energy, and every individual parameter of the PES surface. This global dependence can be used to average the computed observables over variations of the individual PES parameters, as well as over the collision and internal energies in order to produce thermally averaged observables. It can also be used to analyze the influence of the individual PES parameters on the scattering outcome. This makes the model proposed here a unique tool for the analysis of the effects of the PES topology on the molecular scattering dynamics.

Widely used in engineering technologies [13,14], the GP model can be viewed as a technique for interpolation in a multidimensional space. We choose the GP model because it is an efficient nonparametric method. There is no need to fit data by analytical functions so the model is expected to work for any distribution of scattering observables and to become more accurate when trained by more computed observables. Given the scattering observables computed at a small number of randomly chosen points in the multidimensional parameter space, the GP model learns from correlations between the values of these scattering observables to produce a smooth dependence on all the underlying parameters. As an illustrative example, we consider the scattering of benzene molecules C_6H_6 by rare gas (RG) atoms He, Ne, Ar, Kr and Xe. The PES surface for C_6H_6-RG interactions is characterized by eight parameters. We consider two scattering observables [15–17]: the collision lifetimes and the scattering cross sections. We address the following questions. How many scattering calculations are sufficient to train a GP model to produce an accurate global dependence on all the underlying parameters? Can the GP model be used to make predictions of the scattering observables for one collision system based on the known properties of another collision system? Can the GP model be used to characterize the scattering observables near quantum resonances?

We consider a scattering observable $\mathcal{O}$ as a function of q parameters described by the vector $\boldsymbol{x}$. The components of the vector $\boldsymbol{x} = (x_1, x_2, \ldots, x_q)^\top$ can be the collision energy, the internal energy, and/or the parameters representing the PES. We assume that $\mathcal{O}$ is known from a classical or quantum dynamics computation at a small number of $\boldsymbol{x}$ values. Our first goal is to construct an efficient model that, given a finite set of $\mathcal{O}(\boldsymbol{x})$, produces a global dependence of the scattering observable on $\boldsymbol{x}$.

We assume that the scattering observable of interest at any $\boldsymbol{x}$ is a realization of a Gaussian process $F(\cdot)$, characterized by a mean function $\mu(\cdot)$, constant variance σ^2, and correlation function $R(\cdot,\cdot)$. For any fixed $\boldsymbol{x}$, $F(\boldsymbol{x})$ is a value of a function randomly drawn from a family of functions Gaussian distributed around $\mu(\cdot)$. Consequently, the multiple outputs $F(\boldsymbol{x})$ and $F(\boldsymbol{x}')$ at $\boldsymbol{x}$ and $\boldsymbol{x}'$ jointly follow a multivariate normal distribution defined by $\mu(\cdot)$, σ^2, and $R(\cdot,\cdot)$ [18,19]. We assume the following form for the correlation function [20–23]

$$R(\boldsymbol{x},\boldsymbol{x}') = \exp\left\{-\sum_{i=1}^{q}\omega_i|x_i - x_i'|^p\right\} \tag{1}$$

and write

$$F(\boldsymbol{x}) = \sum_{j=1}^{k} h_j(\boldsymbol{x})\beta_j + Z(\boldsymbol{x}) = \mathbf{h}(\boldsymbol{x})^\top\boldsymbol{\beta} + Z(\boldsymbol{x}), \tag{2}$$

where $\mathbf{h} = (h_1(\boldsymbol{x}), \ldots, h_k(\boldsymbol{x}))^\top$ is a vector of k regression functions [24], $\boldsymbol{\beta} = (\beta_1, \beta_2, \ldots, \beta_k)^\top$ is a vector of unknown coefficients, and $Z(\cdot)$ is a Gaussian random function with zero mean. The problem is thus reduced to finding $\boldsymbol{\beta}$, p, and $\Omega = (\omega_1, \omega_2, \ldots, \omega_q)^\top$.

We spread n input vectors $\boldsymbol{x}_1, \ldots, \boldsymbol{x}_n$ evenly throughout a region of interest and compute the desired observable $\mathcal{O}$ at each $\boldsymbol{x}_i$ with a classical or quantum dynamics method. The outputs of a GP at these points $\boldsymbol{Y}^n = (F(\boldsymbol{x}_1), F(\boldsymbol{x}_2), \ldots, F(\boldsymbol{x}_n))^\top$ follow a multivariate normal distribution with the mean vector $\mathbf{H}\boldsymbol{\beta}$ and the covariance matrix $\sigma^2\mathbf{A}$. Here, $\mathbf{H}$ is a $n \times k$ design matrix with the ith row filled with the k regressors $h_1(\boldsymbol{x}_i), h_2(\boldsymbol{x}_i), \ldots, h_k(\boldsymbol{x}_i)$ at site $\boldsymbol{x}_i$, and $\mathbf{A}$ is an $n \times n$ matrix with the elements $\mathbf{A}(i,j) = R(\boldsymbol{x}_i, \boldsymbol{x}_j)$.

Given Ω, the maximum likelihood estimators of $\boldsymbol{\beta}$ and σ^2 have closed-form solutions [11]

$$\hat{\beta}(\Omega) = (\mathbf{H}^\top\mathbf{A}^{-1}\mathbf{H})^{-1}\mathbf{H}^\top\mathbf{A}^{-1}\boldsymbol{Y}^n, \tag{3}$$

$$\hat{\sigma}^2(\Omega) = \frac{1}{n}(\boldsymbol{Y}^n - \mathbf{H}\boldsymbol{\beta})^\top\mathbf{A}^{-1}(\boldsymbol{Y}^n - \mathbf{H}\boldsymbol{\beta}). \tag{4}$$

To find the maximum likelihood estimator of Ω, we fix p and maximize the log-likelihood function

$$\log\mathcal{L}(\Omega|\boldsymbol{Y}^n) = -\frac{1}{2}[n\log\hat{\sigma}^2 + \log(\det(\mathbf{A})) + n] \tag{5}$$

numerically by an iterative computation of the determinant $|\mathbf{A}|$ and the matrix inverse $\mathbf{A}^{-1}$.

The goal is to make a prediction of the scattering observable at an arbitrary $\boldsymbol{x} = \boldsymbol{x}_0$. Because the values $Y_0 = F(\boldsymbol{x}_0)$ at $\boldsymbol{x}_0$ and the outputs at training sites are jointly distributed, the conditional distribution of possible values $Y_0 = F(\boldsymbol{x}_0)$ given the values $\boldsymbol{Y}^n$ is a normal distribution with the conditional mean and variance

$$m(\boldsymbol{x}_0)^* = \mathbf{h}(\boldsymbol{x}_0)^\top\boldsymbol{\beta} + \mathbf{A}_0^\top\mathbf{A}^{-1}(\boldsymbol{Y}^n - \mathbf{H}\boldsymbol{\beta}), \tag{6}$$

$$\sigma^{*2}(\boldsymbol{x}_0) = \sigma^2(1 - \mathbf{A}_0^\top\mathbf{A}^{-1}\mathbf{A}_0), \tag{7}$$

where $\mathbf{A}_0 = (R(\boldsymbol{x}_0,\boldsymbol{x}_1), R(\boldsymbol{x}_0,\boldsymbol{x}_2), \ldots, R(\boldsymbol{x}_0,\boldsymbol{x}_n))^\top$ is specified by the now known correlation function $R(\cdot|\hat{\Omega})$. Equation (6) provides the GP model prediction for the value of the scattering observable at $\boldsymbol{x}_0$.

To illustrate the applicability and accuracy of the GP model, we first compute the collision lifetimes of benzene molecules with RG atoms [25–27]. We use the classical trajectory (CT) method described in Ref. [25]. As shown in Ref. [28], the C_6H_6-RG PES can be expressed as a sum over terms describing the interaction of the RG with the $C-C$ and $C-H$ bond fragments, characterized by eight parameters. We first fix the PES parameters to describe the C_6H_6-Ar system and focus on the dependence of the lifetimes on two parameters: the collision energy E and the rotational temperature T_r. Figure 1 shows the results of the CT calculations, illustrating that the collision lifetime exhibits an inverse correlation with E, while no apparent correlation with T_r. Figure 1(c) shows the global surface of the lifetime as a function of E and T_r obtained from the GP model with $h_1 = 1$, $h_{i>1} = 0$, and p set to 1.95. To quantify the prediction accuracy of the GP model, we calculate the errors $\varepsilon_E = \sqrt{(1/n)\sum_{i=1}^{n}(y_i - \hat{y}_i)^2}$ and $\varepsilon_S = \varepsilon_E/(y_{\max} - y_{\min})$, where y_i are the computed values and $\hat{y}_i$ are the GP model predictions. For the model with only 20 scattering calculations used as training points, $\varepsilon_E = 9.36$ ps and $\varepsilon_S = 7.93\%$. With the number of the scattering calculations increased to 50, the errors decrease to $\varepsilon_E = 5.17$ ps and $\varepsilon_S = 4.38\%$.

The scattering calculations presented in Figs. 1(a) and 1(b) cannot be interpreted to assume any simple functional form. In addition, the vastly different gradients of the T_r

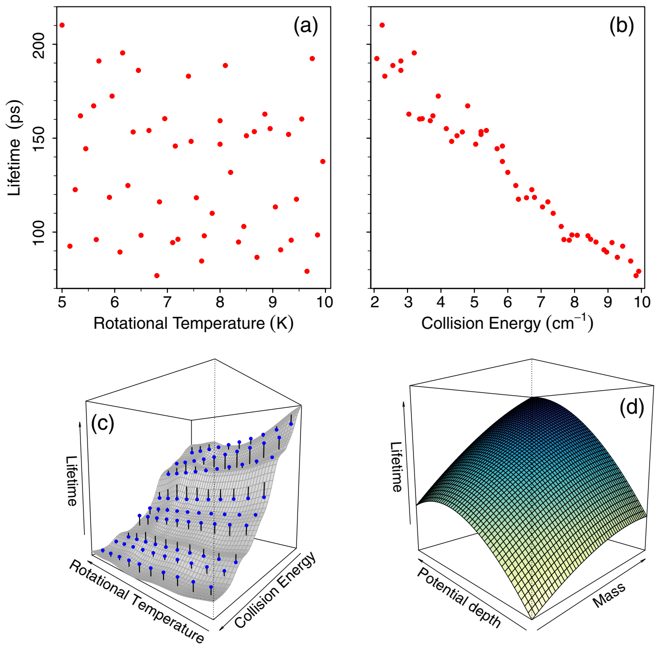

FIG. 1 (color online). (a),(b) The lifetime dependence on the rotational temperature and collision energy for C_6H_6-Ar collisions. (c) The surface produced by the GP model. The lines connect the values (circles) computed from the classical trajectories with the values predicted by the GP model. (d) The surface produced by the GP model for C_6H_6-RG collision lifetimes versus the atomic mass and the PES depth for $T_r = 4$ K and $E = 4$ cm^{-1}. The surface (c) is produced with only 20 scattering calculations on input and has the normalized error $\epsilon_S < 8\%$. The surface (d) is produced with 40 scattering calculations and has the error $\epsilon_S = 5.09\%$.

and E dependence may make the conclusions based on calculations at fixed values of one of the parameters misleading. In contrast, the surface plot in Fig. 1(c) clearly illustrates that the collision lifetimes decrease monotonically with both T_r and E. The effect of the rotational temperature is much weaker especially when $E > 5$ cm^{-1} and there is no strong two-way interaction between T_r and E. The GP model surface can be used to evaluate thermally averaged collision lifetimes by integrating the E dependence at a given T_r.

The GP model can be extended to multiple collision systems for the predictions of the collision properties of a specific collision system based on the known collision properties of another system. To illustrate this, we consider the lifetimes of the long-lived complexes formed by benzene in collisions with the RG atoms He, Ne, Ar, Kr and Xe. As the collision system is changed from the C_6H_6-He system to the C_6H_6-Xe system, there are two varying factors that determine the change of the collision dynamics: the reduced mass and the PES.

As before, we use the GP model $F(\boldsymbol{x}) = \beta + Z(\boldsymbol{x})$ with $\boldsymbol{x}$ now representing the atomic mass μ_A and the interaction strength D_e at the global minimum of the atom-molecule PES obtained by scaling the Ar-C_6H_6 PES. We fix $T_r = 4$ K and $E = 4$ cm^{-1}, and compute the collision lifetimes at 40 randomly chosen points in the interval of μ_A and D_e $[4\text{ g/mol}, 130\text{ g/mol}] \times [80\text{ cm}^{-1}, 520\text{ cm}^{-1}]$, which covers all of the RG-C_6H_6 systems. These 40 calculation points are then used to train the GP model to produce the surface plot shown in Fig. 1(d). The error ϵ_S of the surface is 5.09%. The plot reveals that increasing both μ_A and D_e enhances the collision lifetimes and that the reduced-mass dependence of the collision lifetimes is very weak compared to the dependence on the interaction strength.

The GP model can be exploited to explore the role of the individual PES parameters on the observables. To illustrate this, we now consider that $\boldsymbol{x}$ contains eight parameters giving the analytical form of the RG-C_6H_6 PES [28], in addition to E and T_r. We calculate the lifetimes at 200 randomly selected points in this parameter space and use these points to train the GP model. Figure 2 compares the predicted values with the calculated values for another set

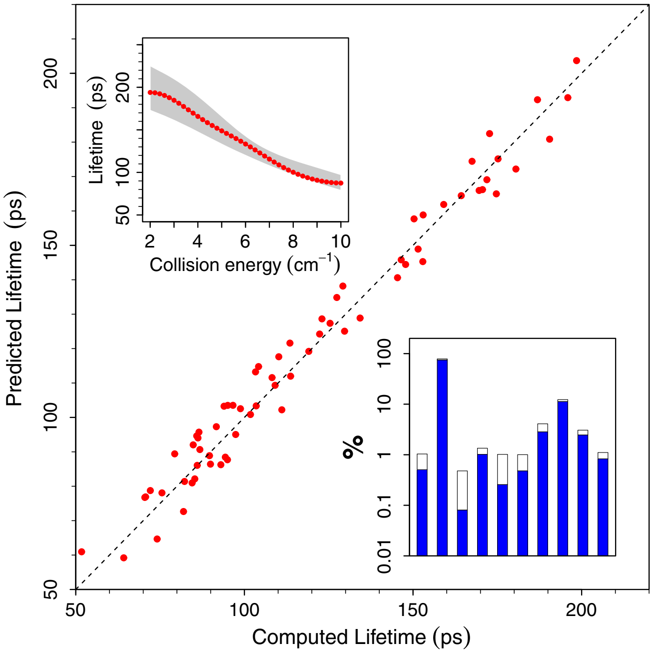

FIG. 2 (color online). Accuracy of the GP model with variable PES parameters for the prediction of the collision lifetimes. The scatter plot compares the predicted values with the computed values. The error of the GP model is the deviation of the points from the diagonal line. This GP model is trained by only 200 scattering calculations, enough to produce a ten-dimensional hypersurface with the error $\epsilon_S = 4\%$. Left inset: energy dependence of the collision lifetime for the Ar-C_6H_6 system with the error interval obtained by varying all the individual PES parameters by $\pm 3\%$. Right inset: relative effect of the variation of T_r, E, and the PES parameters on the collision lifetimes. The filled area of the bars shows the uncorrelated contribution of the corresponding variable and the open area shows the effect that depends on one or more other variables.

of 70 randomly selected points. The plot corresponds to the model error $\varepsilon_S = 4\%$.

The ten-parameter GP model contains a wealth of information on the dependence $\mathcal{O}(\boldsymbol{x})$. For example, one can perform a sensitivity analysis by using the functional analysis of variance decomposition [29–31] to determine which of the PES parameters has the strongest impact on the observable (right inset of Fig. 2). Of the eight PES parameters, the location of the potential well due to the interactions of the RG with the C − C bonds for the parallel approach [28] is the most important factor determining the collision lifetime. The model can also use be used to compute the uncertainties due to global variation of the PES. Figure 2 (left inset) shows the interval of the lifetimes obtained by the simultaneous ±3% variation of all eight PES parameters.

We now consider the applicability of the GP model to quantum scattering calculations. The quantum results are often affected by resonances [2,32], leading to wild variations of the scattering observables in a small range of the underlying parameters. If applied directly to such a case, the GP model is unstable because the steep variation of the correlations leads to singularities in $\mathbf{A}^{-1}$ [33]. This is illustrated in Fig. 3, showing the GP model predictions trained directly by 60 quantum calculations of cross sections for rotationally inelastic He-C_6H_6 scattering, randomly chosen at E between 1 and 10 cm^{-1}. The instability of the GP model arises from the wild variations of the scattering cross sections near resonances. We repeated these calculations for the elastic and state-resolved rotationally inelastic cross sections shown in Figs. 4(a)–4(c) of Ref. [27]. In each case, we found that the wild variation of the quantum results leads to unstable GP model predictions.

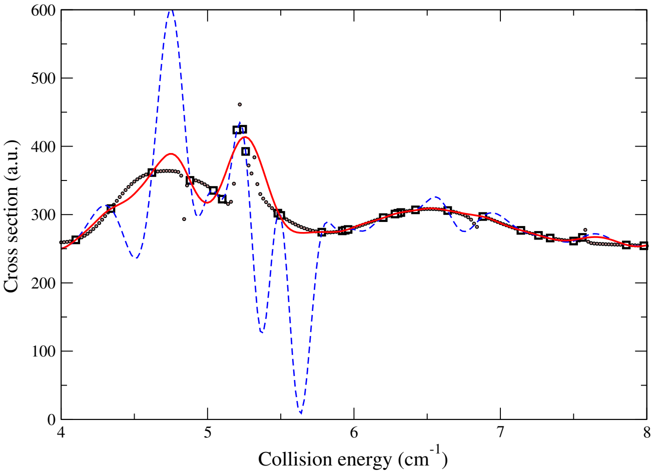

FIG. 3 (color online). GP models (curves) of quantum scattering cross sections (symbols) for C_6H_6-He collisions. The blue dashed line represents the results of the GP model (6) trained by the quantum calculations. The red solid line represents the predictions of the GP model (8) trained by a combination of classical and quantum results. The CT results stabilize the GP model predictions of the quantum calculations. The models are trained by the points represented by squares. The circles are used to illustrate the accuracy.

However, the GP model can be extended to model the time-consuming quantum scattering calculations with the help of efficient classical dynamics calculations. To do this, we introduce a more complex GP as [34]

$$E(\cdot) = \rho F(\cdot) + G(\cdot) + \varepsilon, \tag{8}$$

where $F(\cdot)$ and $G(\cdot)$ are independent Gaussian random functions with $G(\cdot)$ characterizing the difference between the CT and quantum mechanical (QM) calculations and effectively describing the inaccuracy of the classical trajectory method. The calculations are performed in two steps. First, the CT calculations are used to train the GP model $F(\cdot)$. In the second step, the QM and CT calculations are used together to train the model $G(\cdot)$ in Eq. (8), using the parameters of $F(\cdot)$ and treating ρ and ε as variable parameters. This fixes the models $F(\cdot)$ and $G(\cdot)$ as well as ρ and ϵ.

The accuracy of this combined quantum-classical model is illustrated in Fig. 3, showing that the model provides an accurate energy dependence of the cross sections, even near scattering resonances. The CT calculations in a two-function model (8) stabilize the model, removing the errors arising from the resonant variation of the quantum results. We applied the two-step model (8) to the calculations for the elastic and state-resolved rotationally inelastic cross sections shown in Figs. 4(a)–4(c) of Ref. [27] and found a similar improvement in each case.

In summary, we have shown that a Gaussian process model combined with a small number of scattering calculations can be used to obtain an accurate multidimensional dependence of the scattering observables on the experimentally controllable parameters and the PES parameters. Specifically, we showed that the GP model trained only by 20 CT calculations produces a dependence of the C_6H_6-Ar collision lifetimes on the collision energy and the rotational temperature of benzene, with the normalized error $\varepsilon_S < 8\%$. Trained by 200 calculations, the GP model produces a ten-dimensional dependence of the collision lifetimes on the collision energy, the rotational temperature, and eight individual PES prameters, with the error $\varepsilon_S < 4\%$. We have introduced a hybrid GP model that can be trained by a combination of classical and quantum dynamics calculations in order to model the quantum results. We showed that this model works even in the vicinity of quantum scattering resonances, where the direct fit of the quantum results by means of a GP model is unstable. The models described here are expected to find a wide range of applications, from fitting the interaction potentials by solving the inverse scattering problem to analyzing the dependence of scattering observations on external parameters and to calibrating the accuracy of the scattering calculation methods. For example, the inverse scattering problem can be approached with the help of Eq. (8), where $F(\cdot)$ is parametrized by unknown PES parameters and $E(\cdot)$ models the experimental data. The best estimates of the unknown PES parameters can then be found by a Markov-chain Monte Carlo method [35], in a procedure similar to one recently applied in Ref. [36].

We thank Dr. Zhiying Li for allowing us to use her codes for the classical and quantum dynamics calculations. This work is supported by NSERC of Canada.

[1] *Cold Molecules: Theory, Experiment, Applications*, edited by R. V. Krems, W. C. Stwalley, and B. Friedrich (CRC Press, Boca Raton, 2009).

[2] K. Liu, R. T. Skodje, and D. E. Manolopoulos, Phys. Chem. Comm. **5**, 27 (2002).

[3] J. Van Dongen, C. Zhu, D. Clement, G. Dufour, J. L. Booth, and K. W. Madison, Phys. Rev. A **84**, 022708 (2011).

[4] J. L. Booth, D. E. Fagnan, B. Klappauf, K. W. Madison, and J. Wang, Method and device for accurately measuring the incident flux of ambient particles in a high or ultra-high vacuum environment, Google Patents, 2011, U.S Patent No. US 8803072 B2 and Canada Patent No. CA2741772C.

[5] D. Flower, *Molecular Collisions in the Interstellar Medium*, 2nd ed. (Cambridge University Press, Cambridge, England, 2011).

[6] M. D. Frye and J. M. Hutson, Phys. Rev. A **89**, 052705 (2014).

[7] M. L. González-Martínez and J. M. Hutson, Phys. Rev. Lett. **111**, 203004 (2013).

[8] Y. V. Suleimanov, T. V. Tscherbul, and R. V. Krems, J. Chem. Phys. **137**, 024103 (2012).

[9] *Atom-Molecule Collision Theory*, edited by R. B. Bernstein (Plenum, New York, 1979).

[10] N. F. Mott and H. S. W. Massey, *The Theory of Atomic Collisions* (Oxford University Press, New York, 1965).

[11] J. Sacks, W. J. Welch, T. J. Mitchell, and H. P. Wynn, Stat. Sci. **4**, 409 (1989).

[12] C. E. Rasmussen, Gaussian processes in machine learning, in *Advanced Lectures on Machine Learning* (Springer, New York, 2004).

[13] D. Higdon, M. Kennedy, J. C. Cavendish, J. A. Cafeo, and R. D. Ryne, SIAM J. Sci. Comput. **26**, 448 (2004).

[14] D. Higdon, J. Gattiker, B. Williams, and M. Rightley, J. Am. Stat. Assoc. **103**, 570 (2008).

[15] D. Patterson, E. Tsikata, and J. M. Doyle, Phys. Chem. Chem. Phys. **12**, 9736 (2010).

[16] D. Patterson and J. M. Doyle, Phys. Chem. Chem. Phys. (to be published).

[17] D. Patterson, M. Schnell, and J. M. Doyle, Nature (London) **497**, 475 (2013).

[18] R. J. Adler, *The Geometry of Random Fields* (SIAM, Philadelphia, 2010).

[19] H. Cramér and M. R. Leadbetter, *Stationary and Related Stochastic Processes: Sample Function Properties and Their Applications* (Courier Corporation, Mineola, 2013).

[20] T. Mitchell, M. Morris, and D. Ylvisaker, Stoch. Proc. Appl. **35**, 109 (1990).

[21] N. A. Cressie, *Statistics for Spatial Data* (Wiley, New York, 1993).

[22] M. L. Stein, *Interpolation of Spatial Data: Some Theory for Kriging* (Springer, New York, 1999).

[23] M. Abt, Scand. J. Stat. Theory Appl. **26**, 563 (1999).

[24] The regression functions can be fixed as $h_1 = 1$ and $h_{i>1} = 0$.

[25] Z. Li and E. J. Heller, J. Chem. Phys. **136**, 054306 (2012).

[26] J. Cui, Z. Li, and R. V. Krems, J. Chem. Phys. **141**, 164315 (2014).

[27] Z. Li, R. V. Krems, and E. J. Heller, J. Chem. Phys. **141**, 104317 (2014).

[28] F. Pirani, M. Albertí, A. Castro, M. Moix Teixidor, and D. Cappelletti, Chem. Phys. Lett. **394**, 37 (2004).

[29] G. Pujol, Sensitivity: Sensitivity Analysis, R package version 1.4–0 (2008).

[30] A. Saltelli, M. Ratto, T. Andres, F. Campolongo, J. Cariboni, D. Gatelli, M. Saisana, and S. Tarantola, *Global Sensitivity Analysis: The Primer* (Wiley, New York, 2008).

[31] O. Roustant, D. Ginsbourger, and Y. Deville, J. Stat. Softw. **51**, 1 (2012).

[32] C. Chin, R. Grimm, P. Julienne, and E. Tiesinga, Rev. Mod. Phys. **82**, 1225 (2010).

[33] R. K. S. Hankin, J. Stat. Softw. **14**, 1 (2005).

[34] M. Kennedy and A. O'Hagan, J. R. Stat. Soc. Ser. B **63**, 425 (2001).

[35] W. K. Hastings, Biometrika **57**, 97 (1970).

[36] J. Novak, K. Novak, S. Pratt, J. Vredevoogd, C. E. Coleman-Smith, and R. L. Wolpert, Phys. Rev. C **89**, 034917 (2014).